Presentation 1

DYNAMIC APERTURE FOR LEP: Physics and Calculations

By J.M. Jowett

1.1 Introduction

In the past year our understanding of the physical phenomena determining the dynamic aperture of LEP has evolved considerably. New physics has been introduced in our model of the single particle dynamics in the storage ring. Now particles can be tracked through the structure with a satisfactory inclusion of radiation effects, realistic distributions of the RF cavities, etc. This is particularly important for LEP as single-particle dynamics at LEP2 will be dominated by radiation effects and the discrete RF distribution.

In this talk I shall discuss how the radiation effects have been incorporated and illustrate how they modify the behaviour of particles. The physical mechanisms leading to particle loss are quite different from those which determine the dynamic aperture in proton (or lower-energy electron) rings. I shall also describe how our tracking methodology has evolved to provide a better exploration of phase space and tools for the analysis of the behaviour of particles. Other consequences of the new approach are the removal of arbitrary number of turns, the calculation of phase-space distribution functions and the modelling of measurements (such as those involving coherent excitation of the beam). Finally, I shall present some tracking results for the dynamic apertures of LEP at different energies and in different optical configurations, with and without the inclusion of radiation. I hope to convince you that we are now moving towards a realistic description of single-particle dynamics, better agreement with measurements and, most importantly, improved predictions for LEP2.

1.1.1 Concept of Dynamic Aperture

The idea of dynamic aperture is evoked schematically in Figure ??. The motion of particles around the ring is described as a map from the space of the 6 phase space coordinates at a given azimuth $s = 0$ (deviations from closed orbit and conjugate momenta) onto itself. For LEP, the observation point $s = 0$ is usually IP1.

A working definition,with no pretensions to rigour, can be given as follows: The *dynamic aperture* is the largest connected region of single-particle phase space (around the closed orbit) in which particle motion remains bounded or, better, does not reach amplitudes corresponding to the physical boundary in (x, y, t) space (collimators, vacuum chamber).

1.1.2 Non-radiating particles

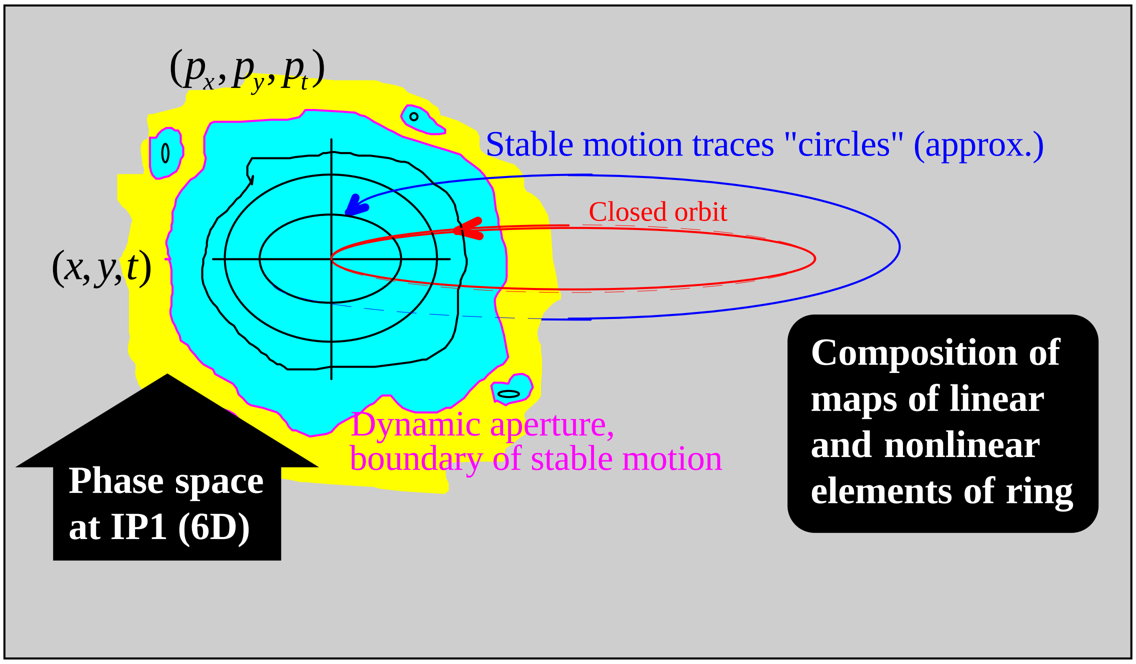

Figure 1.1: Schematic concept of dynamic aperture.

The relation of the fundamental equations of motion to a tracking program such as MAD [?] is shown schematically in Figure ??. In the absence of radiation, particles are lost by some combination of the familiar mechanisms which generate instability in a Hamiltonian system:

- Chromatic effects in which the dependence of the betatron tunes on momentum deviation δ, brings them onto a resonance: $Q_x = p$ or $Q_y = p$, with $p \in \mathbb{Z}$.
- Nonlinear resonances driven by non-linearities, $k_x Q_x + k_y Q_y + k_s Q_s = p$ with $k_x, k_y, k_s, p \in \mathbb{Z}$, leading to beating or unstable growth of amplitudes.
- Chaotic instabilities resulting from the combination of many resonances.
- Modulation of machine parameters by sources such as power supply ripple.

For proton machines it is difficult to decide when to stop tracking as losses can occur by effects which build up over very long times: dynamic aperture estimates can depend on the number of turns tracked. This is sometimes expressed by the use of "survival plots".

1.1.3 Synchrotron radiation

1.1.3.1 Radiative time scales Electrons, on the other hand, radiate photons which change their energy as they traverse magnetic fields. The photons are emitted at random times and with random energies. The statistical properties of these two random variables depend on the instantaneous momentum of the particles and on the local magnetic field. In terms of the primitive canonical variables shown in Figure ??, the magnetic field depends on the two transverse coordinates x and y and the independent variable s. The relevant properties of synchrotron radiation are recalled in Figure ?? using the notations and formalism developed in [?].

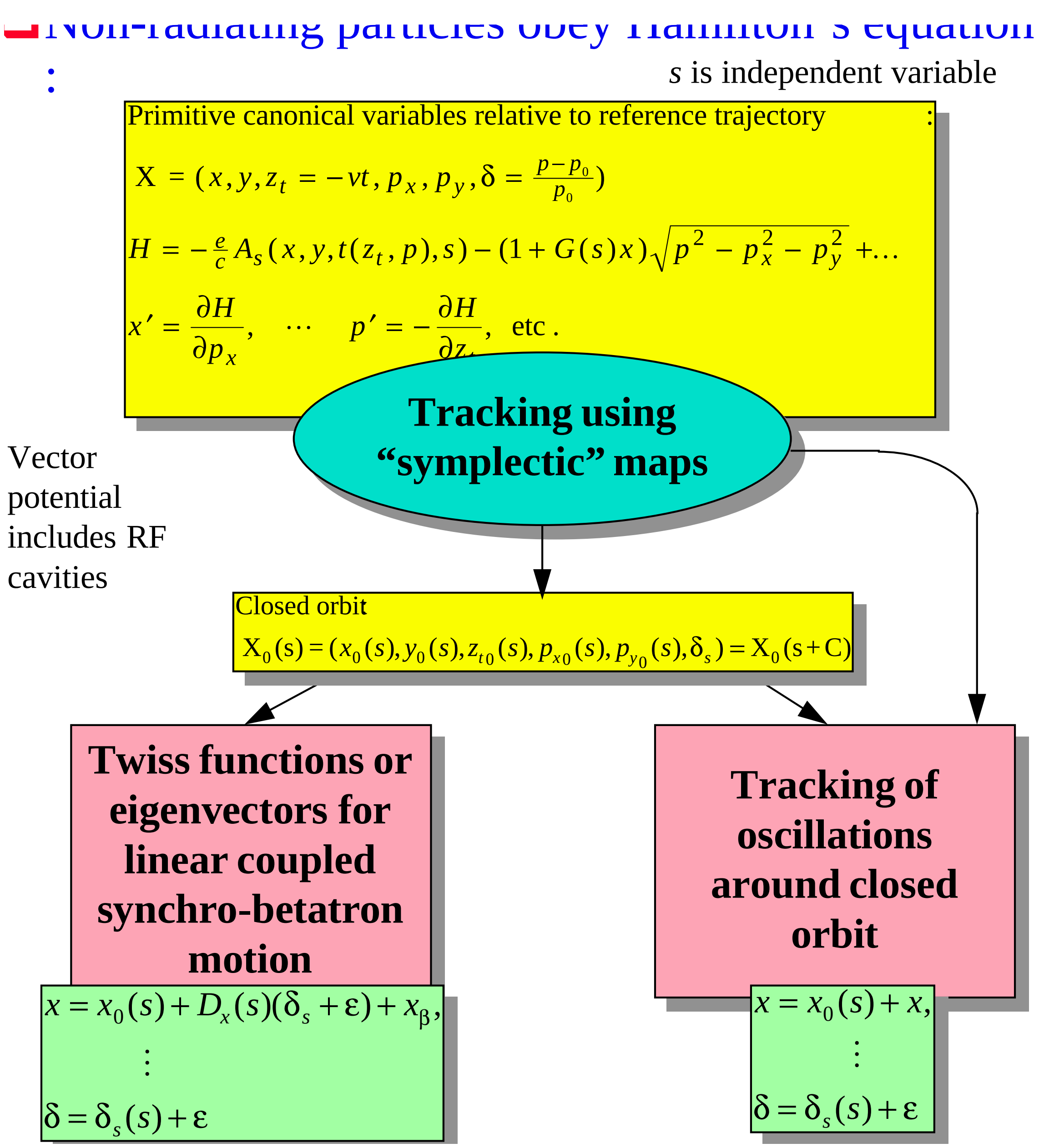

Figure 1.2: Schematic description of how the fundamental equations of motion of a particle in a magnetic field are transformed to generate a tracking program in a neighbourhood of the closed orbit in a synchrotron or storage ring. N.B. the equilibrium momentum deviation $\delta_s(s)$ (which, in hadron machines, is usually a constant) is a component of the closed orbit (determined by RF frequency).

Random emission time *and* photon energy

Density of a given realisation

$$\Omega_X(u,s) = \sum_j \delta(s-s_j)\delta(u-u_j), \quad \langle \Omega_X(u,s) \rangle = N_X(s) f_X(u;s)/c$$

$$N_X(s) = \text{photon emission rate} = \frac{5\sqrt{3}}{6}\frac{cr_e p_0}{\hbar} b_X(s)$$

$$f_X(s) = \text{energy spectrum of photons}$$

Instantaneous radiation power

$$\boxed{P_X(s) = c\sum_j u_j \delta(s-s_j),}$$

$$\langle P_X(s) \rangle = N_X(s)\langle u \rangle_X = c_1 c^2 p^2 b_X(s)^2$$

$$\langle u \rangle_X = \text{mean photon energy} = \frac{8}{15\sqrt{3}} u_c = \frac{4}{5\sqrt{3}}\frac{\hbar c p_0}{(mc)^3} p^2 b_X(s)$$

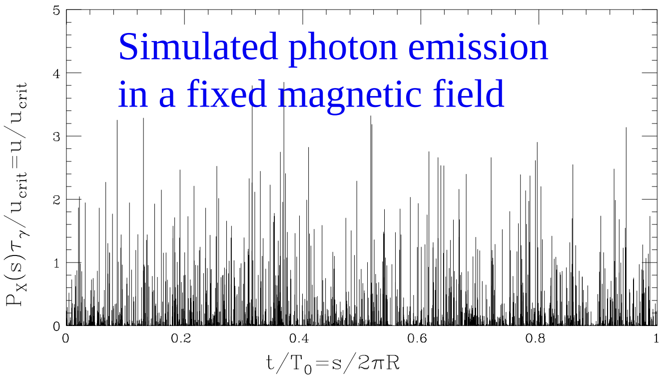

$$c_1 = \frac{2r_e p_0^2}{3(mc)^3}, \quad b_X(s) = \frac{e}{p_0 c}|\mathbf{B}(x,y,s)| \qquad \langle \xi(s)\xi(s') \rangle = \delta(s-s_j)$$

Stochastic representation of fluctuating power

$$P_X(s) = c^2 p^2 \left(c_1 b_X(s)^2 + \sqrt{c_2 b_X(s)^3}\,\xi(s) \right)$$

Figure 1.3: Basic properties of synchrotron radiation and the representation of the instantaneous power as a stochastic process following [?]. Representation of power can be approximated or simplified (with loss of some physics) in various ways (examples later).

Averaging over the emission of discrete photons, synchrotron radiation leads to the radiation damping of betatron and synchrotron oscillations. With respect to this average picture, the quantum fluctuations of the true photon emission give rise to a diffusion which opposes the radiation damping. The beam finds an equilibrium between the two, usually characterised by a gaussian distribution of amplitudes.

These phenomena are of course well known and have been encountered in many electron rings previous to LEP. However they will be much stronger at LEP2 than in previous machines, including the present LEP1. This is illustrated in Figure ?? which shows dimensionless quantities characterising the strengths of radiation damping (τ_x/T_0 is the number of turns per damping time) and quantum excitation per turn over the operating ranges of LEP and PEP. It is striking to notice that, at LEP2, the radiation damping time will be just a few tens of turns. With this and the rapid diffusion from quantum excitation we can expect the effects of many resonances to be masked.

Radiation damping per turn : $$\frac{T_0}{\tau_X} = \frac{\langle P_X \rangle}{E} \propto \frac{E^3}{\rho},$$

Quantum excitation per turn : $$\frac{N_X \langle u^2 \rangle T_0}{E^2} = \frac{4\sigma_\varepsilon^2}{\tau_x / T_0} \propto \frac{E^5}{\rho^2}$$

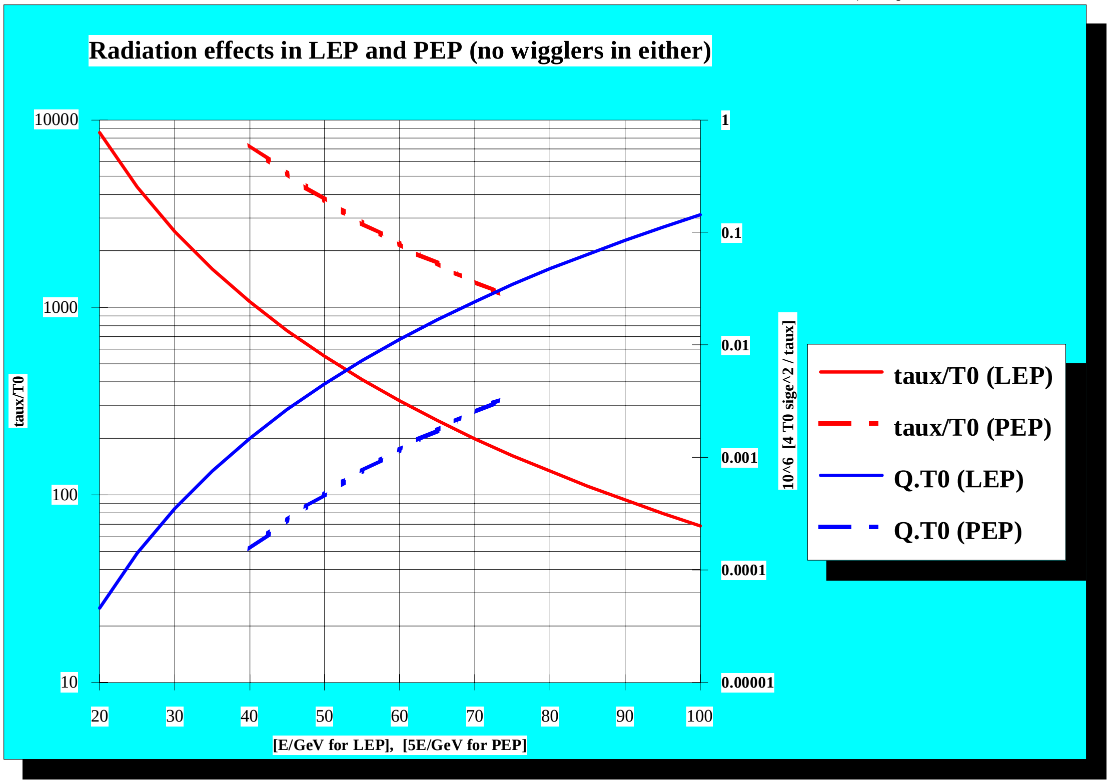

Figure 1.4: Variation of quantities characterising synchrotron radiation over the operating ranges of PEP and LEP.

D:\CHAM4\GENPERF1\PORBRF0.XLS 08:55 07/02/94

COMMEN' **LEP2: w05v6, 90 GeV, e+ orbit, ideal RF**

DATE	22/12/93
TIME	15.13.03
GAMTR	76.6922
ALFA	1.70E-04
XIY	1.60461
XIX	1.53416
QY	76.186
QX	90.2695
CIRCUM	26658.87
DELTA	0
TYPE	OPTICS
ORIGIN	MAD,8.13/11,HP/UX

Ideal LEP2 RF configuration with 192 SC cavities, 120 Cu cavities.
Example of energy sawtooth and closed orbit, which contains additional terms beyond that given directly by energy sawtooth (Bassetti effect):

$$x_c(s) = 0 + D_x \delta_s(s) + x_B(s)$$

NAME	X	DX	PT	DX*Pt	X-DX*PT
IP1	0.003028	-0.016967	0.477586	-0.008103	0.011132

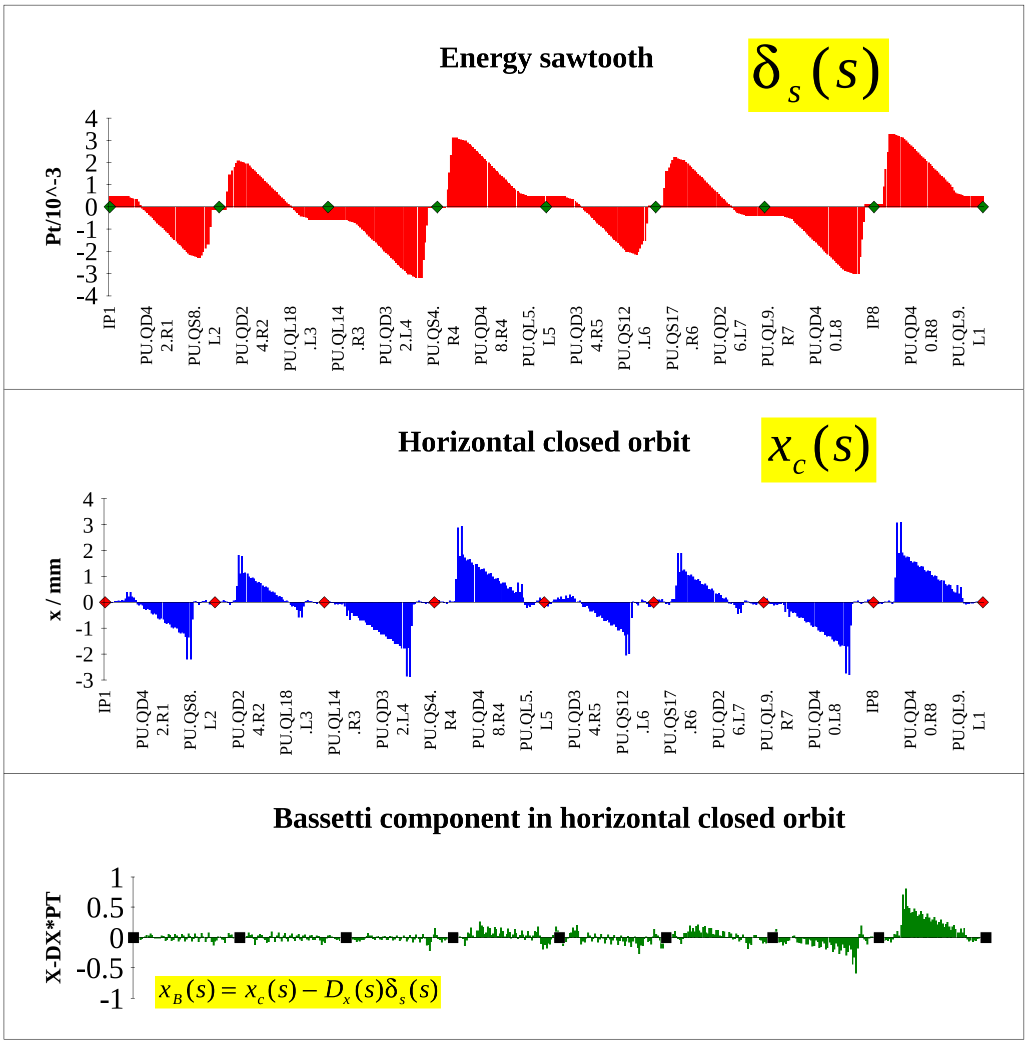

Figure 1.5: Positron energy sawtooth, orbit and Bassetti term at 90 GeV with ideal RF configuration.

1.1.3.2 Energy sawtooth The local variation of the average beam energy (down in magnets, up in RF cavities) gives rise to the phenomenon of the "energy sawtooth", a local variation of the energy/momentum component of the closed orbit, which is different for the electrons and positrons. It follows that the bending, focussing and nonlinearities, will be different leading to locally different closed orbits, Twiss functions and dynamic aperture for the two beams.

Figure ?? shows the variation of the central momentum deviation $\delta_s(s)$ for an ideal LEP2 RF configuration (the energy gains around IP4 and IP8 are higher than at IP2 and IP6 where Cu cavities are installed) at 90 GeV. The horizontal closed orbit contains a component which can be related to $\delta_s(s)$ through the local dispersion function. However it also contains another small component [?] which is shown in the bottom part of the figure.

1.2 Tracking Radiating Particles

Figure ?? is a modification of Figure ?? for the case of radiating particles. Suitable radiation reaction terms can be constructed [?] and added to Hamilton's equations to take full account the discrete photon emission. The equations of motion are now stochastic differential equations and are no longer Hamiltonian. The advantages of canonical transformation theory for transforming the equations of motion into other sets of coordinates can be preserved by a formalism which allows the dissipative terms to be transformed using matrices derived from the generating function [?].

In practice, you do not always want to track with the full representation of the radiation power. As described in the following subsections, various simplifications can be made. Each of them corresponds to a mode of tracking which is available in MAD [?].

1.2.1 Symplectic tracking with no radiation

Representation of radiation power	**MAD commands**
$P_X(s) \quad = 0$	`BEAM,particle=positron,Energy=20.,-radiate` `TRACK`

Most of the particle tracking done for other machines, and—sufficiently far back in the past—for LEP, simply ignored the radiation. This may be an acceptable approximation in cases where the radiation terms are small. It is certainly not acceptable for LEP except, possibly, at its injection energy of 20 GeV. If radiation terms are not included at all, the quadratic terms in the Hamiltonian (which determine the linear betatron and synchrotron oscillations, the small-amplitude tunes, etc.) will be wrong. The most obvious manifestation of this occurs when synchrotron oscillations are included[1]. If radiation terms are not 0included, then the particle does not find the proper stable phase. In the full 6-dimensional description, the stable phase-angle is just one component of the closed orbit. Moreover, the focussing functions (which include the RF) must be defined on the true closed orbit. Thus in such a case, the particle has incorrect tunes.

[1]Many older tracking programs are transverse-optics-oriented and do not attempt to even include synchrotron motion properly. Sometimes they simply modulated the momentum of the particles (which defines the transfer maps of the transverse coordinates through a magnetic element) at the desired synchrotron frequency. The present MAD generates the synchrotron oscillations naturally by accelerating the particles with the voltages they would experience according to the phase of their arrival time at a cavity with respect to that cavity's own frequency and phase lag relative to a universal clock. Each cavity can have its own frequency and lag [?]. The stable phase angle—if there is one—is found by the closed-orbit-finding algorithm.

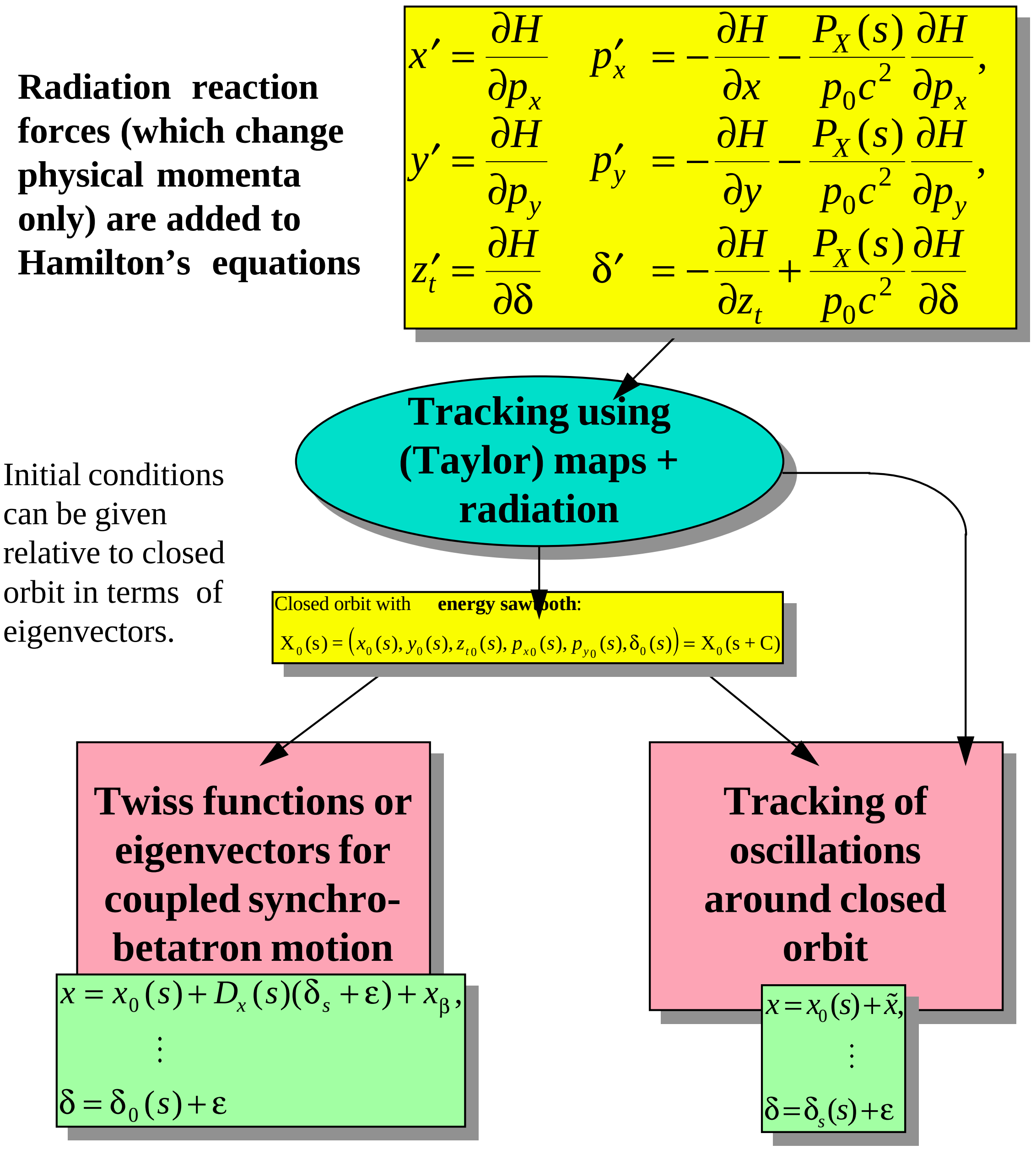

Figure 1.6: Tracking scheme for radiating particles. N.B. the momentum deviation, $\delta_s(s)$, on the closed orbit includes the systematic losses by radiation in magnets and gains from the RF (sawtooth).

1.2.2 Symplectic tracking with radiation

Representation of radiation power	MAD commands
$P_X(s) \quad = c^2 p_0(s)^2 c_1 b\,(x_0(s), y_0(s), s)^2$	`BEAM,particle=positron,Energy=90.,radiate` `TRACK,-damp`

It can be proved mathematically[2] that is possible to consider symplectic maps around the closed orbit (i.e., including stable phase angle, energy sawtooth, etc.) determined by radiation. Each particle has exactly the same energy loss, namely the energy lost by a particle on the closed orbit. This includes, for example, the additional energy lost in when the closed orbit passes off-centre through a quadrupole. Thus, can have your cake without baking it: the tunes of small betatron and synchrotron oscillations around the closed orbit will be correct but there will be no radiation damping—the system will remain Hamiltonian.

Older versions of MAD (i.e., those released before the summer of 1993) performed a sort of tracking with radiation in which each particle lost just the energy which a particle of *constant nominal energy would have lost in the dipoles*. The representation of the radiation power was effectively $P_X(s) = c^2 p_0^2 c_1 b\,(0, 0, s)^2$ where p_0 is just the constant reference momentum. This led to an incorrect sawtooth orbit although the stable phase angle was approximately correct in most cases. The tracking was Hamiltonian but the calculations of radiation damping, emittances, etc. were incorrect when the closed orbit went off-centre in quadrupoles.

Figure **??** illustrates the difference between symplectic tracking without radiation (described in Section **??** above) and the symplectic tracking with radiation described in this section.

Figure **??** is an example of one kind of behaviour that can be seen in symplectic tracking with radiation in the neighbourhood of a synchro-betatron resonance.

1.2.3 Tracking with radiation damping

Representation of radiation power	MAD commands
$P_X(s) = c^2 p^2 c_1 b\,(x, y, s)^2$	`BEAM,particle=positron,Energy=90.,radiate` `TRACK,damp`

This mode of tracking includes the dependences of the classical (deterministic) radiation power on all the canonical variables in all magnetic elements. There is a continuous loss of energy and modification of the particle momenta. The dependence of $P_X(s)$ on the canonical variables is precisely the origin of radiation damping.

This mode of tracking has been the most used recently for the study of LEP2 optics and most of the results to be presented in this talk.

It is striking that the dynamics becomes relatively simple and utterly different from the symplectic model (see Figure **??** for a generic example): particles with large betatron amplitudes are damped rapidly back to the closed orbit. They simply do not stay long enough at large amplitude for the effects of high-order resonances to build up as they do in symplectic tracking. The dynamic aperture becomes independent of number of turns and the number of turns necessary is small (we have found that everything is over within the first 30 turns at 90 GeV!). The particle is either lost quickly or damps down to the closed orbit.

[2] Starting from the equations of motion in Figure ?? and making a canonical transformation to variables relative to the closed orbit.

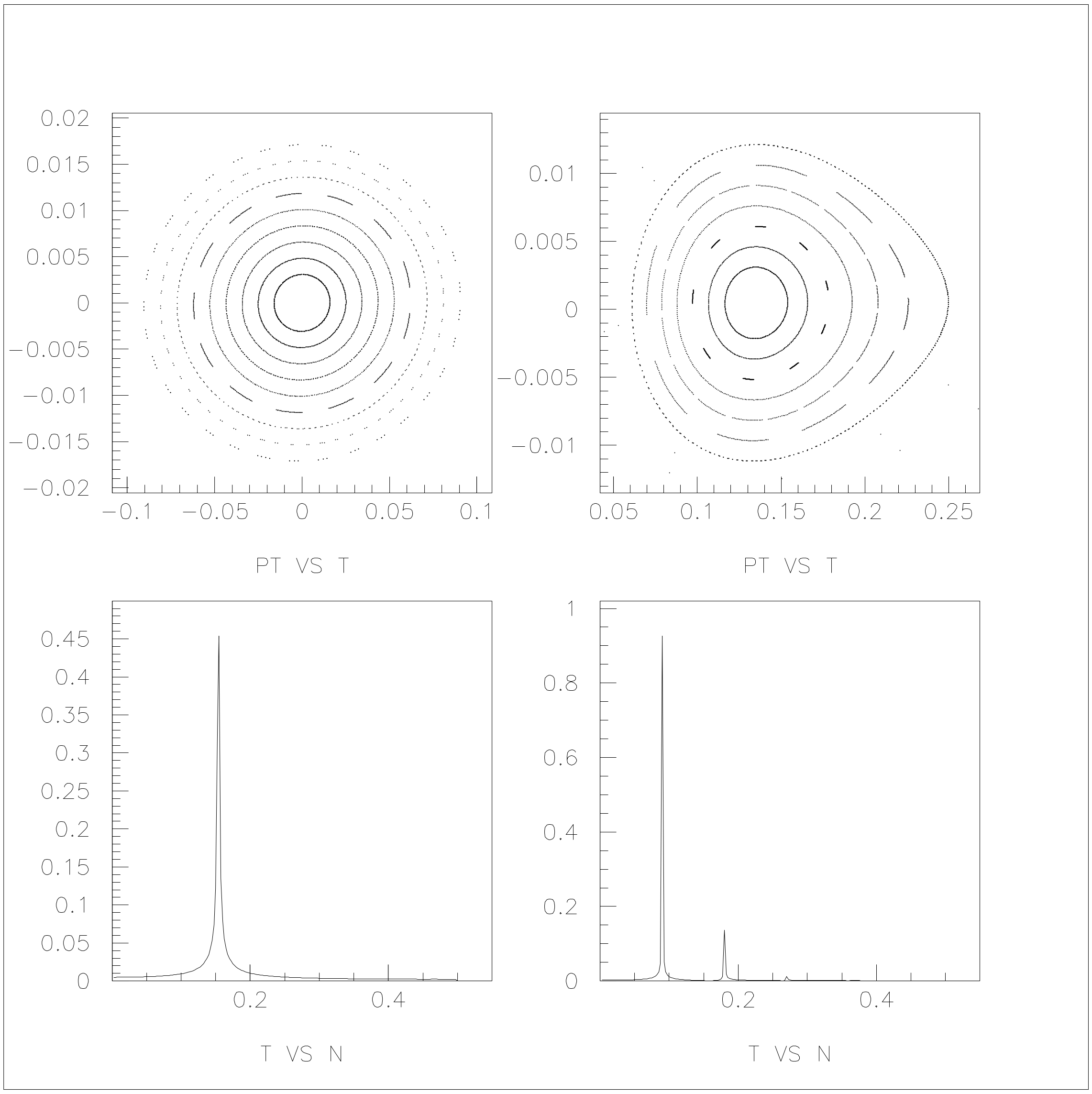

Figure 1.7: Two ways of tracking a LEP2 optics with 90°/60° phase advances at 90 GeV with the nominal RF configuration (192 superconducting (SC) and 120 Cu cavities). The left-hand plots show the synchrotron phase space (for several particle orbits) and a Fourier spectrum (for a single particle) in an example of *symplectic tracking without radiation* (described in Section ??). The particles have no initial betatron amplitudes. In this case the particles oscillate around a stable phase of 0° where the RF restoring potential is symmetric and the synchrotron tune Q_s is higher than it should be.
The plots on the right correspond to *symplectic tracking with radiation* (described in Section ??). Now the closed orbit includes the correct stable phase angle and gives the correct value of Q_s.

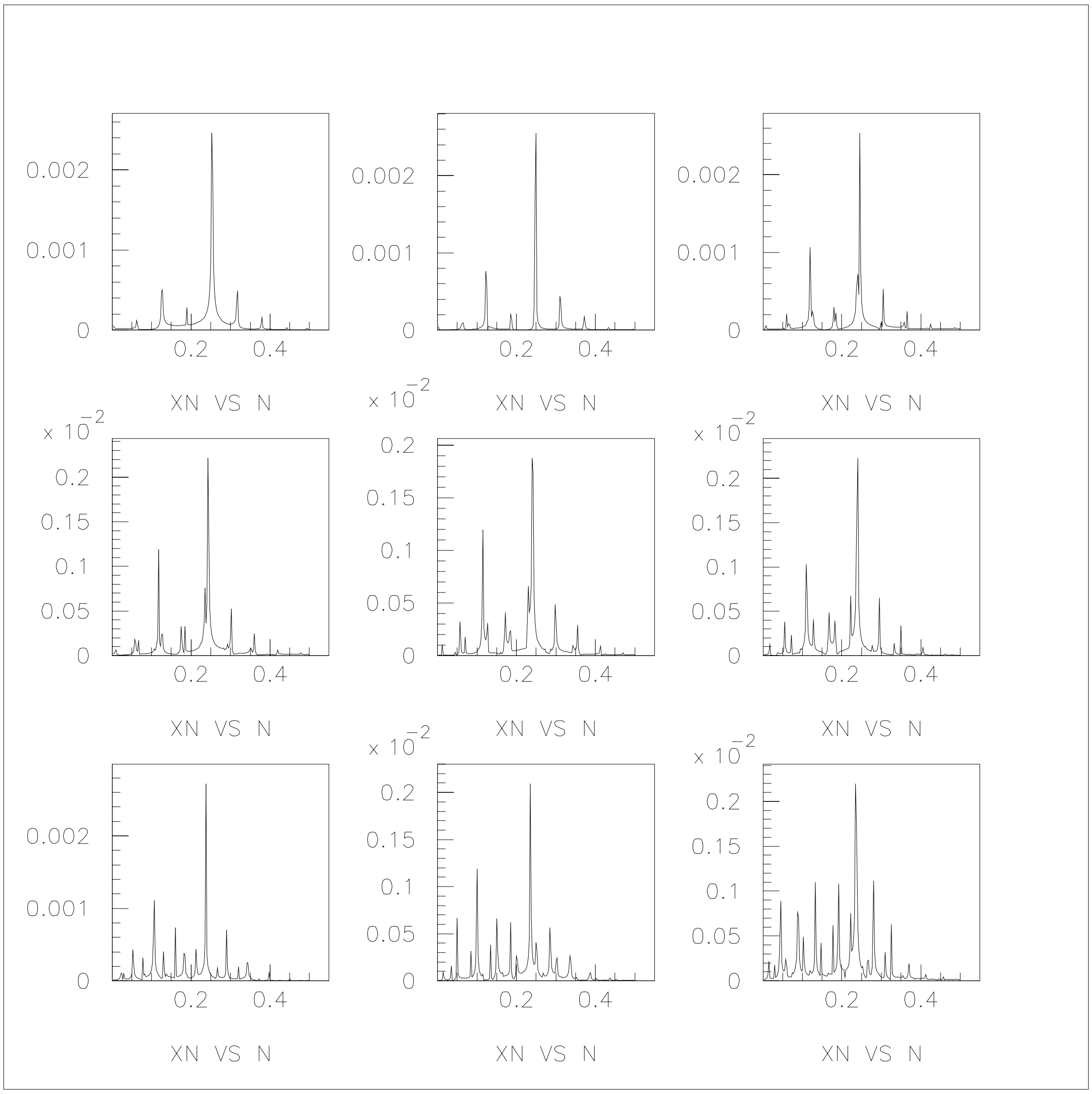

Figure 1.8: Symplectic tracking with radiation in the LEP1 90°/60° optics that was used for physics in 1993 at 45.6 GeV, with the standard configuration of 120 Cu RF cavities around IP2 and IP6, The plots show the spectrum of horizontal betatron motion for a range of synchrotron amplitudes from zero up to 1.5 % and illustrate the increasing influence of coupling due to the synchro-betatron resonance: $Q_x - 4Q_s = 76$.

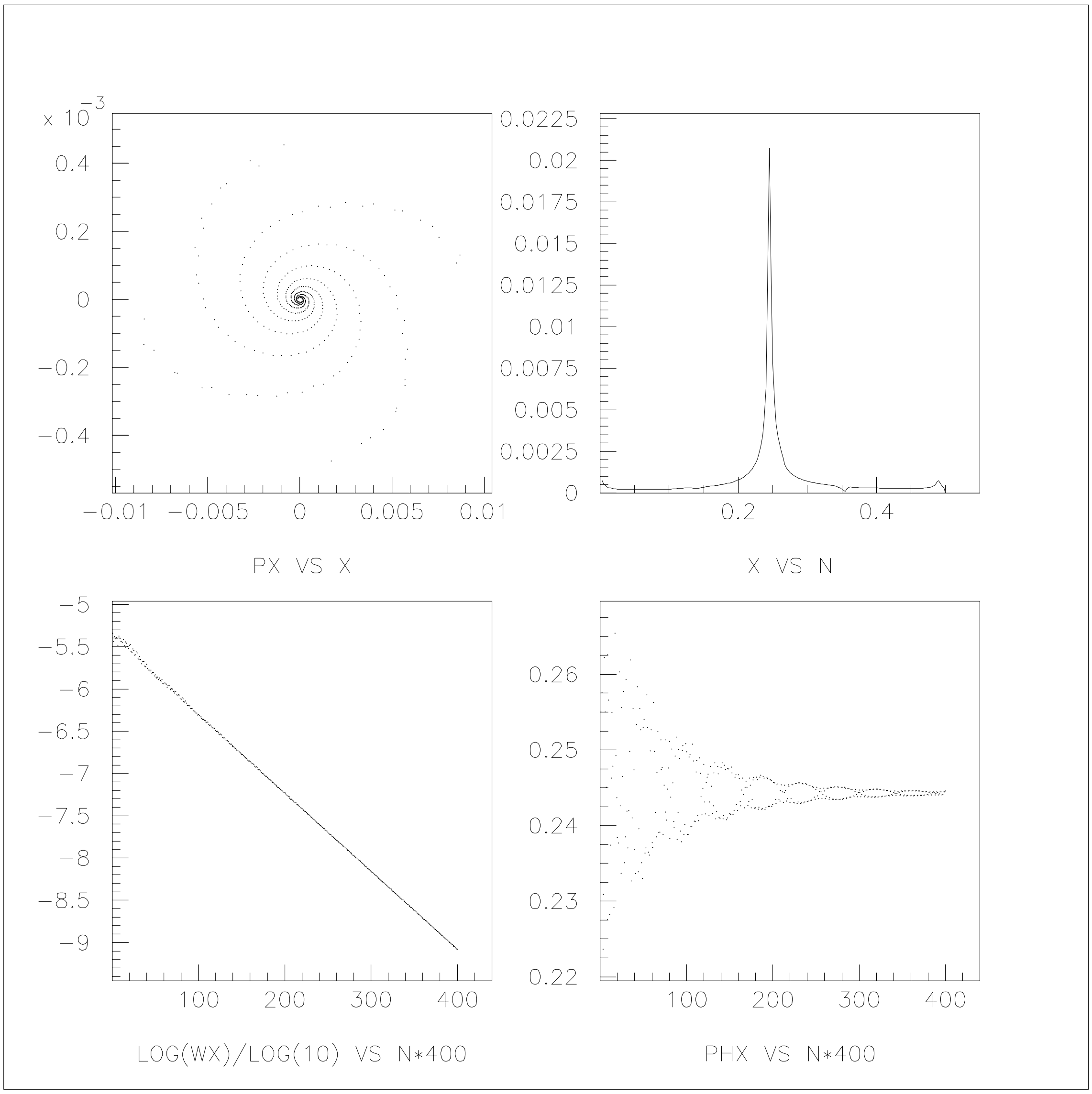

Figure 1.9: Tracking with radiation damping for a LEP2 90°/60° optics at 90 GeV with 192 superconducting (SC) + 120 Cu cavities and no initial synchrotron amplitude. Clockwise from top left: (i) rapid damping of betatron amplitude to the closed orbit, (ii) spectrum of transverse motion shows a single (broadened) line at the betatron tune, (iii) the phase advance per turn rapidly settles to the value corresponding to the tune (iv) the logarithm of the action variable vs. the turn number shows clean exponential damping. The MAD tracking reproduces the correct damping time.

1.2.4 Tracking with Quantum Emission

Representation of radiation power	MAD commands
$P_X(s) = c\sum_j u_j\delta(s-s_j)$ $= c^2p^2\left(c_1 b(x,y,s)^2 + \sqrt{c_2 b(x,y,s)^3}\xi(s)\right)$	`BEAM,particle=positron,Energy=90.,radiate` `TRACK,quantum`

The ultimate tracking mode simulates the true random photon emission as well as we know how, in order to simulate quantum fluctuations as well as damping. Formally it uses the complete representation of the stochastic radiation power as described in Figure ??.

The algorithm for simulating photon emission [?, ?, ?] goes essentially as follows:

1. Decide how many photons to emit in an element of length L and normalised magnetic field $b(x,y,s)$, according to a Poisson distribution with mean $N_X(s)L/c$.
2. Generate a random energy for each photon according to the photon distribution for synchrotron radiation (the universal form for the distribution in units of the critical energy which scales with momentum p and magnetic field $b(x,y,s)$.
3. Modify the three components of the particle's momentum (in MAD, this is actually done at the entrance and exit of each element).

All phenomena related to radiation (the closed orbit, damping, energy spread, emittance, change of damping partition with $f_{\rm RF}$, the gaussian (or other!) phase-space distribution, etc., arise from these photons. No parameter (such as the damping time or emittance) is inserted "by hand".

With the introduction of randomness, of course, the tracking becomes a kind of "Monte-Carlo" simulation.

A generic example of tracking with photon emission is shown in Figure ??.

Figure ?? provides a more interesting example of a non-gaussian distributions close to a resonance.

1.3 Tracking Methodology

Together with the improvements in the model of single-particle dynamics described in the previous section, a number of improvements have been incorporated in the procedure for evaluating the dynamic aperture:

Analysis of tracked orbits New software to display and analyse the orbits tracked by MAD (many phase-space projections, FFTs, fits to particle distributions, evolution of action variables in time, etc.) is very useful in understanding the physical processes which lead to instability.

3D dynamic aperture scans Scans of the dynamic aperture were formerly done in only two dimensions (usually $\sqrt{A_x}$ vs. $\sqrt{A_t}$ with the constraint that $\sqrt{2A_y} = \sqrt{A_x}$). Now they are being done in (the square roots of) the action variables of the three normal modes using a standard protocol for a semi-automated scan (moving outwards along rays in action space).

Tracking done with radiation damping Most tracking is done with radiation damping. Occasionally symplectic tracking around the sawtooth closed orbit is used. Tracking with quantum fluctuations (which becomes a Monte-Carlo) will require a new definition of dynamic aperture.

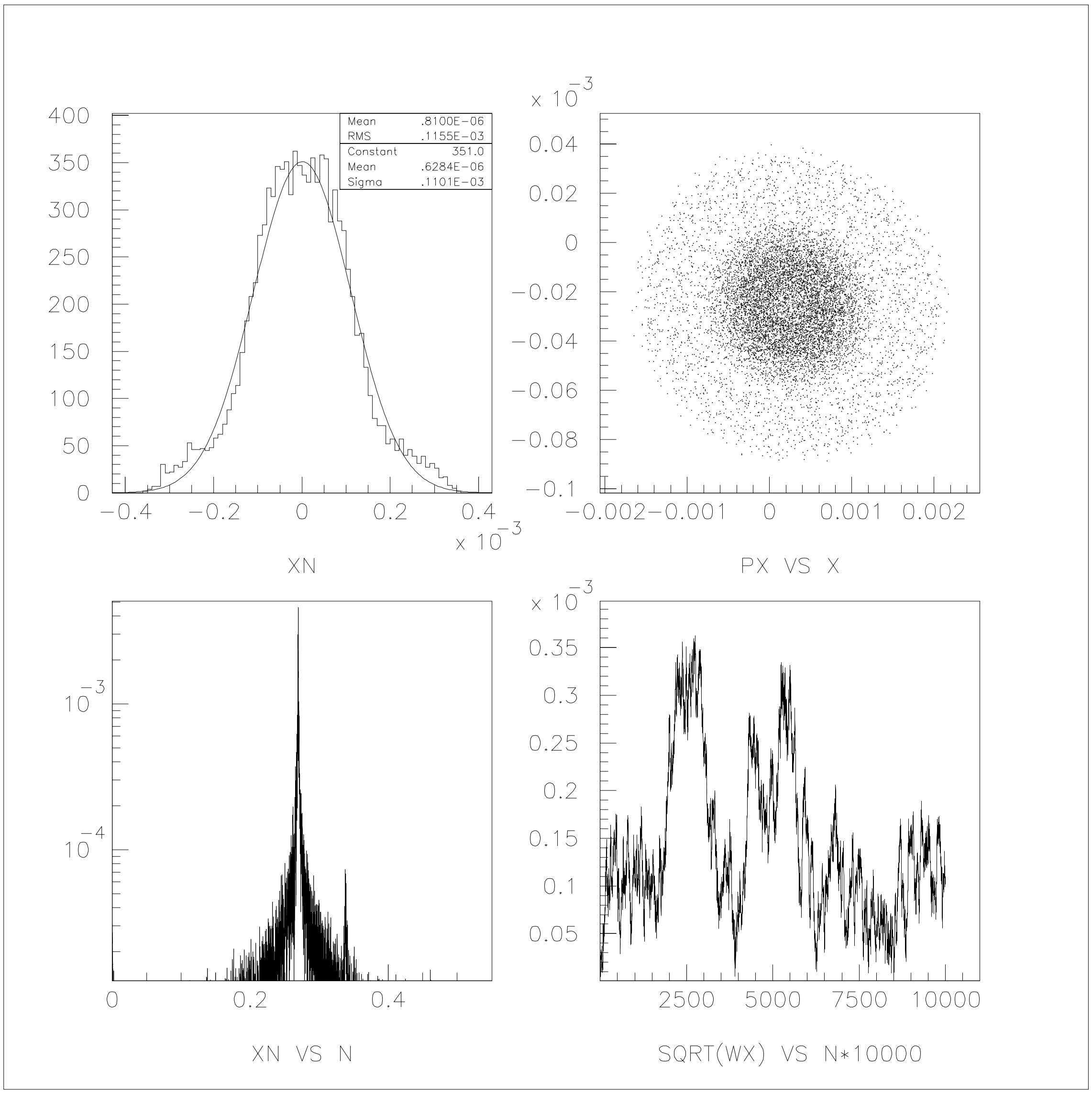

Figure 1.10: Betatron motion and spectrum by tracking with quantum emission in the 1993 physics optics at 45.6 GeV with the standard LEP1 configuration of 120 Cu cavities. A single particle is started on the closed orbit and tracked for 10000 turns. Clockwise from top left: (i) averaged over time, the orbit reproduces the correct natural emittance and gaussian distribution of amplitudes in the horizontal normal mode (betatron motion), (ii) the scatter plot in betatron phase space, (iii) the betatron amplitude executing a “random walk” as a function of the turn number, (iv) the Fourier spectrum of the orbit shows a single peak at the tune.

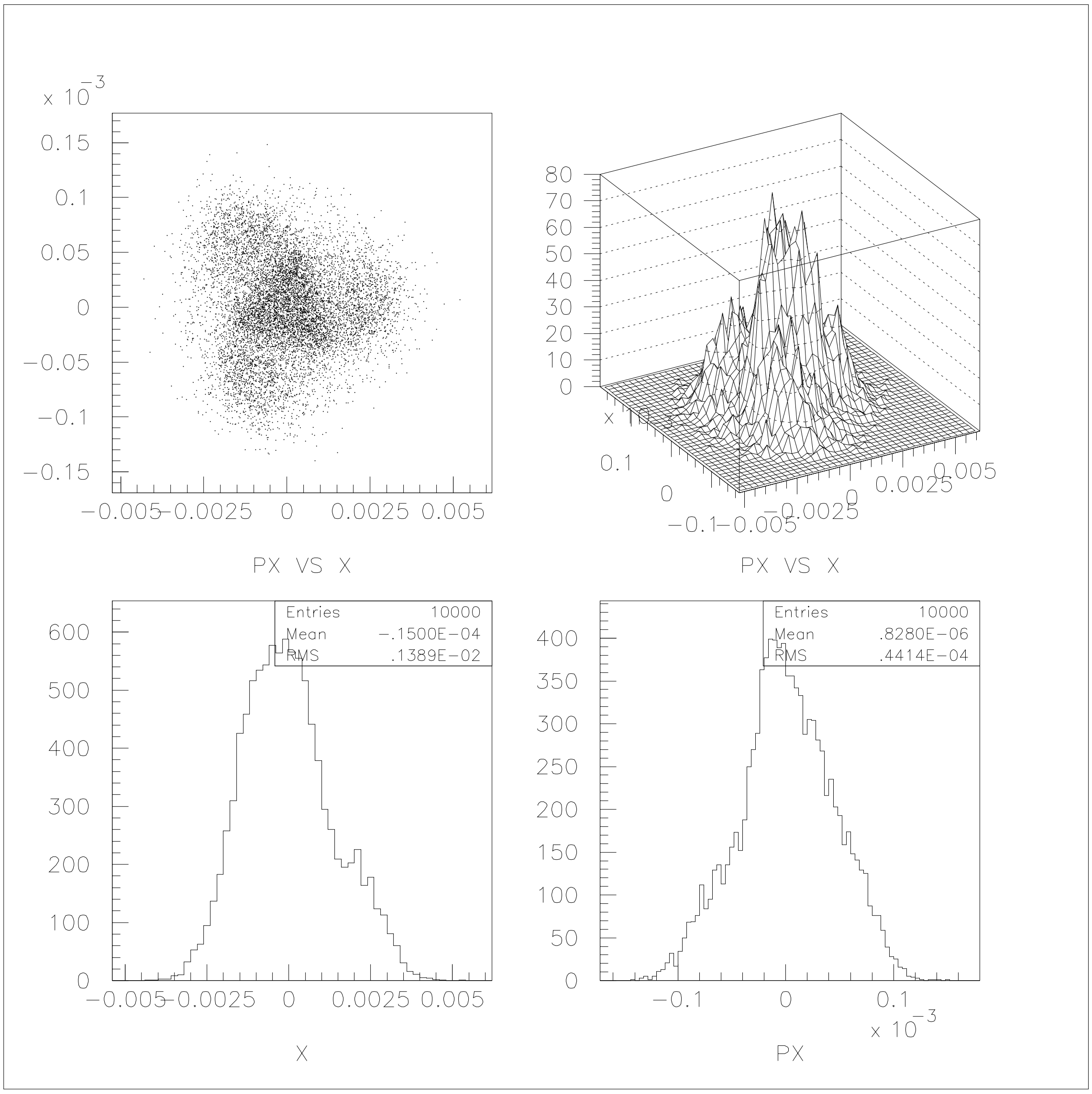

Figure 1.11: Betatron motion and spectrum by tracking with quantum emission in a LEP2 135°/60° (low-emittance) optics at 90 GeV with the nominal 192 superconducting (SC) plus 120 Cu cavities. The tune, $Q_x = 125.35$, is placed close to a third-integer resonance. Again, a single particle is started on the closed orbit and tracked for 10000 turns. Clockwise from top left: (i) the scatter plot in betatron phase space, showing the triangular form of what would be the separatrix in the single-resonance approximation of the underlying Hamiltonian system. The detuning with amplitude creates three islands surrounding stable period-3 fixed points. There is a constant flux of particles into and out of these islands. Particles being damped down from large amplitudes can move around them to reach the closed orbit or can be trapped temporarily in them. (ii) the density of the orbit can be used to construct the distribution in phase space, of which projections onto the (iii) momentum coordinate and (iv) coordinate axes clearly show the non-gaussian character and density enhancement around the period-3 fixed points.

Full LEP2 RF system in real layout Tracking is now being done with the full set of 120 Cu and 192 superconducting (SC) cavities in their proper positions, with appropriate voltages. The voltage distribution for LEP2 never has complete fourfold symmetry, as can be seen Figure ??. Since there are individual voltage parameters for each klystron, we can also study the effects of RF trips, etc.

Dynamic aperture independent of number of turns As was pointed out above, at high energy with strong damping, the dynamic aperture becomes independent of the number of turns tracked. This removes a troublesome ambiguity from the estimate of dynamic aperture.

Vacuum chamber boundary In reality particle losses occur on the metal of the vacuum chamber. This is represented in every quadrupole of the machine as a "collimator", i.e., a physical amplitude which, once reached, defines the particle as lost. It would be meaningless to include particles which made bounded oscillations wholly or partly outside the chamber.

Imperfections Machine imperfections can be included systematically. There has not been time to do much tracking like this.

Modelling of coherent excitation It is possible to model the Q-meter kicker to understand experiments which try to measure the dynamic aperture by exciting a coherent excitation of the beam. We have found the phenomena which occur to be rather complex and the procedures necessary to study the beam-response functions are tricky even on the computer. These studies will be described elsewhere and are summarised in [**?**].

1.3.1 Variables and Units

I should explain the "invariant units" in which I shall present the dynamic aperture results. The have the advantage of being independent of beam size (sometimes people use the number of "σs"), hence energy, in a fixed optics without radiation effects. They are actually the *canonical actions of the small amplitude normal modes* (i.e., the action variables of the linear dynamical system in the neighbourhood of the closed orbit). To avoid introducing the notation of normal-mode eigenvectors [?], let me just say that, in the simplest situation, when the motion is uncoupled (except for purely horizontal dispersion), the variables

$$\left(10^3\sqrt{[A_x/\mathrm{m}]}, 10^3\sqrt{[A_y/\mathrm{m}]}, [\sqrt{A_t}/\%]\right) \tag{1.1}$$

are related to the primitive canonical variables through

$$\begin{aligned} x &= \sqrt{2\beta_x(s)A_x}\cos\left(2\pi Q_x s/C + \mu_x(s) + \phi_x\right) \\ &\quad + D_x(s)\left(\delta_s(s) + \sqrt{A_t}\cos\left(2\pi Q_s s/C + \mu_s(s) + \phi_s\right)\right) \\ y &= \sqrt{2\beta_y(s)A_y}\cos\left(2\pi Q_y s/C + \mu_y(s) + \phi_y\right) \end{aligned} \tag{1.2}$$

It is helpful to remember that, with these restrictions,

- $(10^3\sqrt{[A_x/\mathrm{m}]}$ is the maximum amplitude of betatron oscillations in mm at a place where $\beta_x = 1\,\mathrm{m}$ (similarly for A_y) and
- $[\sqrt{A_t}/\%]$ is THE maximum amplitude of synchrotron oscillation in energy expressed in % of momentum deviation.

Initial conditions for tracking are expressed in terms of these quantities. Complete coverage of the 6-dimensional phase space would require a variation of the conjugate angle variable (phase) but this is impractical and often not necessary (phases generally mix quickly—but there are couterexamples) and these are generally taken as 0 or $\pi/2$.

1.4 Dynamic Aperture of LEP1

1.4.1 Ideal machine

Figure ?? shows the results of tracking with radiation damping for the 1993 LEP injection configuration at 20 GeV and the physics configuration at 45 GeV. In both cases, the machine is assumed to be perfect. Comparing the dynamic aperture surface with the one which indicates the beam size, it is clear that the LEP1 beams are comfortably accommodated in the dynamic aperture.

1.4.2 Effect of Misalignments

The dynamic aperture measured in 1992 [?] was found to be smaller than in 1993 and, apparently, than it was in 1989-91. It is natural to ask whether this could discrepancy could have been due to the (now) known bad misalignment of the machine in 1992. A test of this hypothesis has been made[3] by tracking the 1992 injection optics at 20 GeV, with and without the inclusion of the misalignments measured in the 1992–93 survey. Radiation damping was included and the damping wigglers were switched on.

$[\sqrt{A_t}/\%], \phi_t$	$(0.004, \pi)$	$(0.002, \pi)$	$(0, 0)$	$(0.002, 0)$	$(0.004, 0)$	
$\max 10^3\sqrt{[A_x/\mathrm{m}]}$	2.9	3.1	3.5	3.1	2.9	(ideal machine)
$\max 10^3\sqrt{[A_x/\mathrm{m}]}$	2.4	2.9	3.2			(misaligned)

Table 1.1: Tracking results, effect of misalignments

The results of this tracking, shown in Table ??, show that the misalignments do indeed reduce the dynamic aperture. However the conclusion is that the change in dynamic aperture generated by the misalignments is insufficient to explain the measured discrepancy.

1.4.3 Effect of Damping (LEP1)

Before radiation damping was implemented properly in tracking, it was often argued that tracking without radiation damping was a reasonable approach since it would give pessimistic results with respect to the stability of particles. Damping, it was (naïvely?) expected, can only improve stability.

This expectation is confirmed by the comparison shown in Figure ??. Further comparisons will be made in Section ??.

In passing, please note that the effects of radiation at LEP1 are significant and should always be taken into account.

1.5 Dynamic Aperture of LEP2

In this section, I shall present some results for LEP2 at 90 GeV.

[3] The results and conclusion of this section are due to A. Verdier.

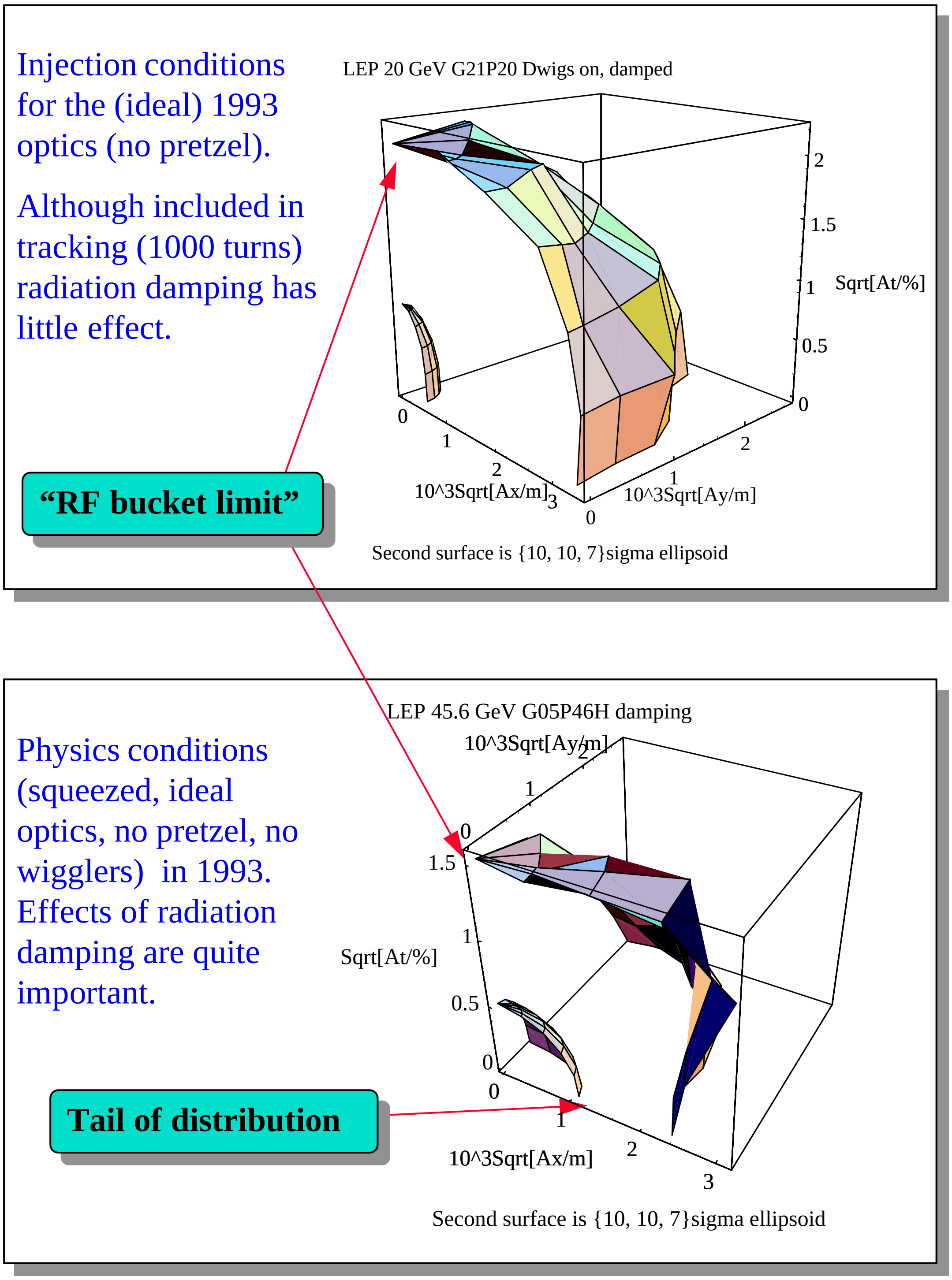

Figure 1.12: LEP1 Dynamic Aperture at 20 GeV (G21P20 optics) and in the standard physics conditions (G05P46H optics) at 45.6 GeV. The inner surface shown on each plot is an ellipsoid with semi-major axes equal to $(10\sqrt{\epsilon_x}, 10\sqrt{\epsilon_y = \epsilon_x/2}, 7\sigma_\epsilon)$, i.e., it represents a "$(10,10,7)\sigma$" contour of the beam. This is not, of course, a contour of constant density but a convenient indication of the "beam-stay-clear" that we would like inside the dynamic aperture.

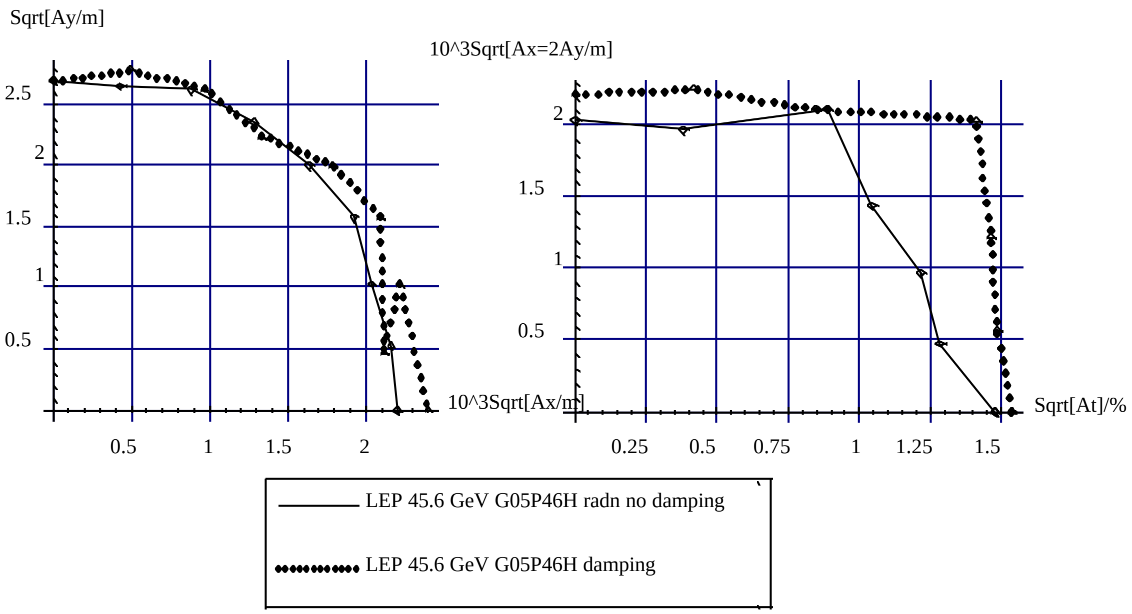

Figure 1.13: Two cuts of the dynamic aperture of the 1993 physics optics, showing the effect of adding radiation damping in the tracking. In both cases, the tracking is done around the sawtooth closed orbit.

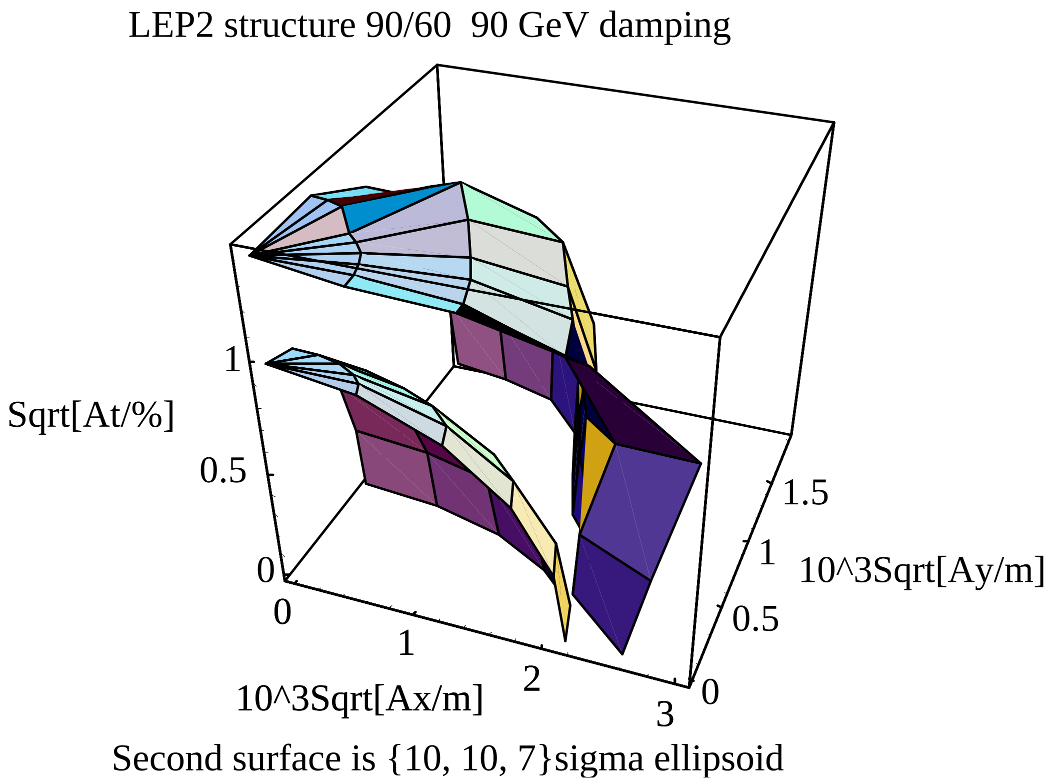

Figure 1.14: Dynamic aperture of a 90°/60° optics for LEP2 at 90 GeV with Q_s=0.114. The tracking includes radiation damping, the sawtooth, the nominal LEP2 RF configuration (192 superconducting (SC) + 120 Cu cavities) etc. but no imperfections or quantum fluctuations. The beam-stay-clear surface is shown in the same manner as in Figure ??.

1.5.1 LEP2 90°/60° optics

Figure ?? shows the dynamic aperture for a typical LEP2 optics (although not quite the latest version) and can be compared directly with the LEP1 results shown in Figure ??. Various two-dimensional sections of the same dynamic aperture are shown in Figure ??.

Comparing with Figure ??, shows that, although the dynamic aperture is roughly the same size, much more of it will be used since the beam emittances are larger. This dynamic aperture would be *just barely adequate in the horizontal plane.*

1.5.2 Effect of Damping at LEP2

Figure ?? shows the results of an exercise similar to that of Section ??. In this case the naïve expectation that damping should improve the dynamic aperture is not borne out: the limit of stability for vertical betatron oscillations is reduced significantly when damping is included in the tracking.

1.5.3 Comparison of LEP2 optics

The dynamic apertures of three potential LEP2 optics are compared in Figure ??. In each case the tracking is done in the same way (with damping) and the same RF configuration. Only the customary "fully-coupled" cut of the dynamic aperture is shown and you should remember that other cuts may look different. The three optics are roughly similar in terms of dynamic aperture.

1.6 Loss Mechanisms with Radiation

Analysis of tracked orbits has revealed new loss mechanisms when radiation is included. Particles are still, of course, lost because of chromatic effects, e.g., the variation of Q_y with momentum and synchrotron amplitude remains important. Other resonances, synchro-betatron couplings and modulations, non-linear dispersion, etc. all play their rôles.

Here I shall briefly describe a new effect which I propose to call **Radiative Beta-Synchrotron Coupling** (RBSC). It is a *non-resonant* effect. A particle with a large betatron amplitude make an extra energy loss by radiating in quadrupoles. If you imagine that its betatron amplitude does not change much over a number of synchrotron oscillations (this is not essential to the effect), you can say that its "effective stable phase angle" will change to reflect the greater energy loss. The particle will tend to oscillate about a displaced fixed point in the synchrotron phase plane. This results in a growth of the oscillation amplitude which may eventually lead the particle outside the stable region *in synchrotron phase space.*

μ_x/μ_y	I_{6x}	I_{6y}
90°/60°	76.81	221.01
135°/60°	106.79	149.96

Table 1.2: Comparison of radiation integrals for quadrupoles in some LEP2 physics optics. Note that the low-β insertion quadrupoles make important contributions to these integrals.

This effect is important in determining the transverse dynamic aperture at LEP2 energies and is responsible for the reduction in dynamic aperture found when damping was included in Section ??.

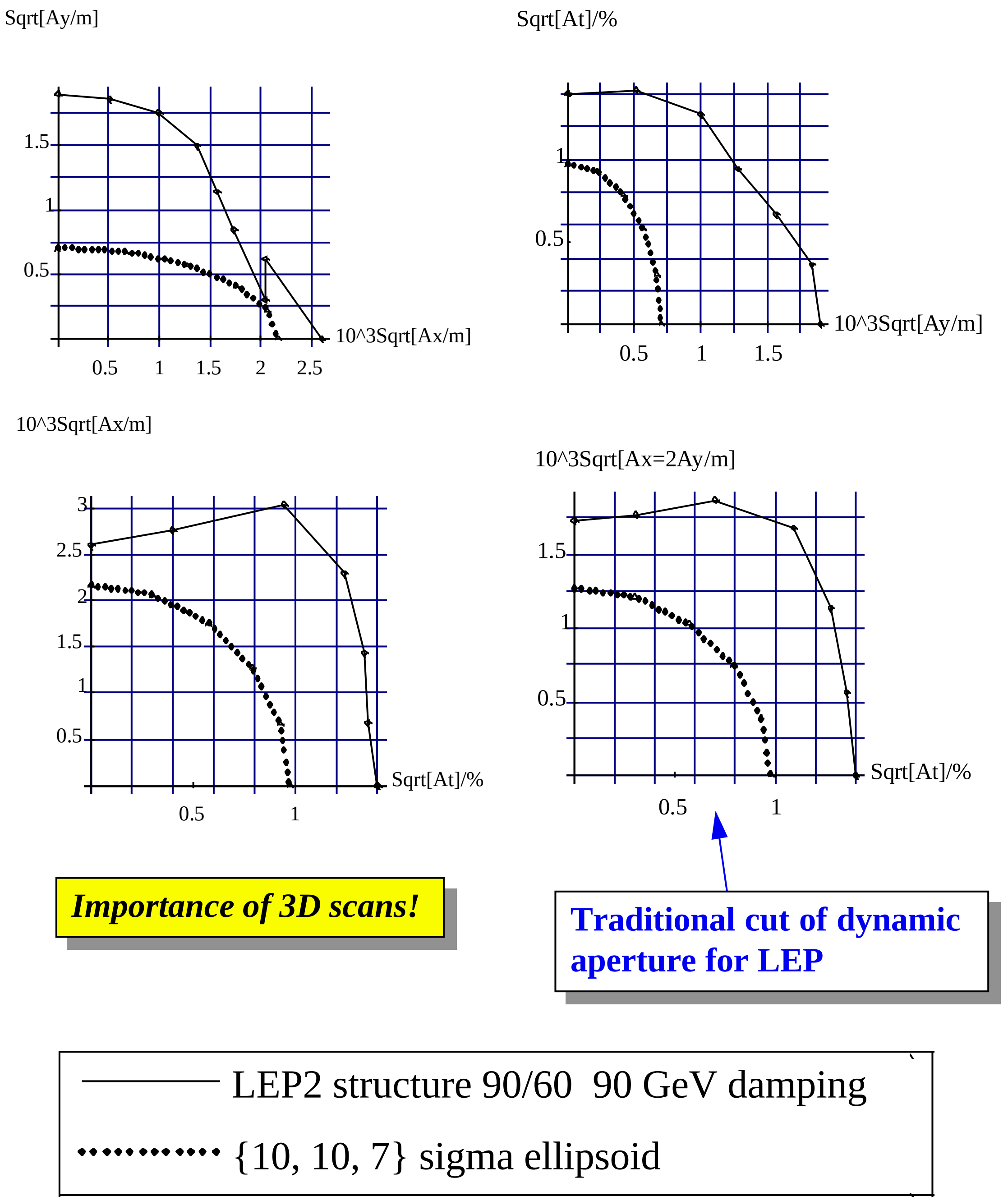

Figure 1.15: Two-dimensional cuts of the dynamic aperture shown in Figure ??.

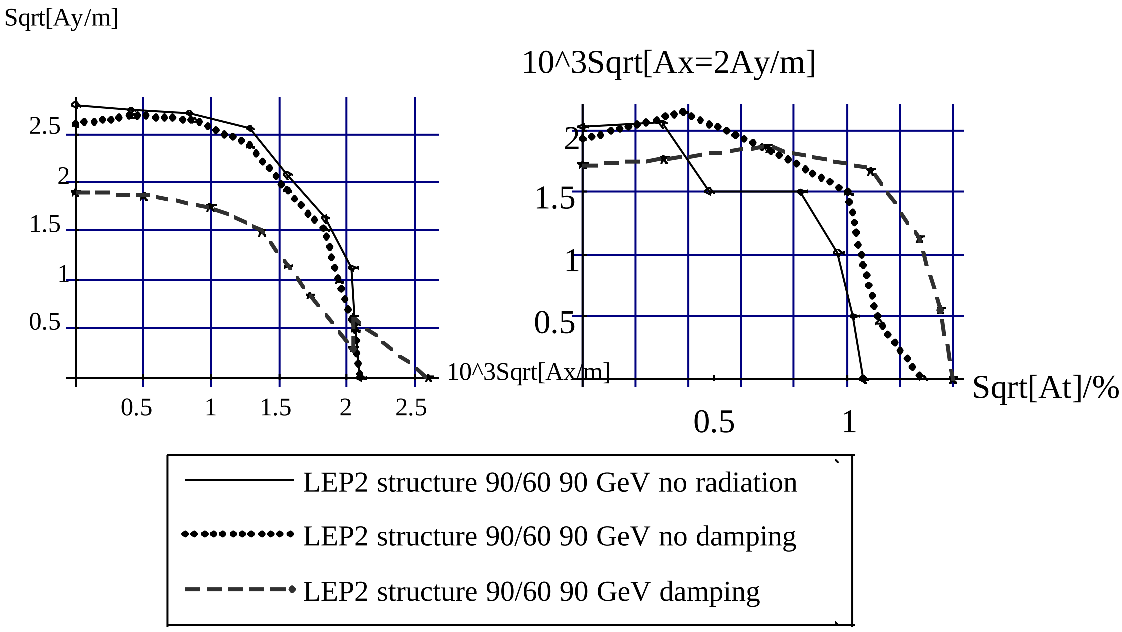

Figure 1.16: Effect of including radiation in the closed orbit and of including damping at 90 GeV. In each case, exactly the same optics is used but the tracking mode is changed.

Its magnitude is determined by the synchrotron radiation integrals:

$$I_{6x} = \int K_x^2(s)\beta_x(s)\,ds, \qquad I_{6y} = \int K_y^2(s)\beta_y(s)\,ds, \tag{1.3}$$

(see Table ??).

As a rough estimate of the effect we can calculate the shift in effective stable phase angle

$$\begin{aligned} \Delta\phi_s &\approx \arcsin\left(\sin\phi_{s0}\frac{U_{\text{dipoles}} + U_{\text{quads}}}{U_{\text{dipoles}}}\right) - \phi_{s0} && (1.4)\\ &\approx \tan\phi_{s0}\frac{U_{\text{quads}}}{U_{\text{dipoles}}} && (1.5)\\ &\approx \tan\phi_{s0}\frac{I_{6x}A_x + I_{6y}A_y}{I_2} && (1.6) \end{aligned}$$

where the last approximation holds for sufficiently small A_x and A_y.

Figure ?? shows an example of a particle which experiences this effect quite strongly but remains stable nevertheless. In Figure ??, you can see an example of how RBSC generates instability.

1.7 Conclusions

- Single-particle dynamics in LEP at high energy is strongly influenced by radiation effects.
- Tracking is now much more realistic because these effects are included in what appears to be a fully satisfactory and physically correct fashion. Moreover the model of the machine is better (RF, vacuum chamber, misalignments, etc.)

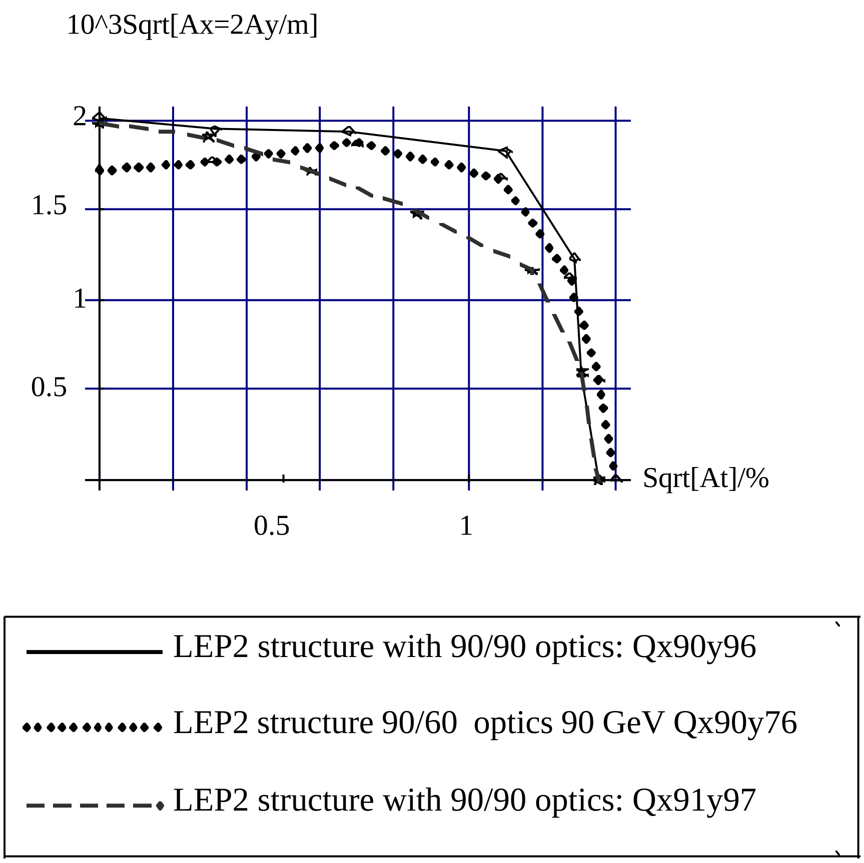

Figure 1.17: Comparison of 3 LEP2 optics: (i) a pretzel optics with $\mu_x = \mu_y = 90°$, (ii) a pretzel optics with $\mu_x = 90°$, $\mu_y = 60°$ and (iii) another optics with $\mu_x = \mu_y = 90°$ but with phase advances in appropriate for the pretzel scheme.

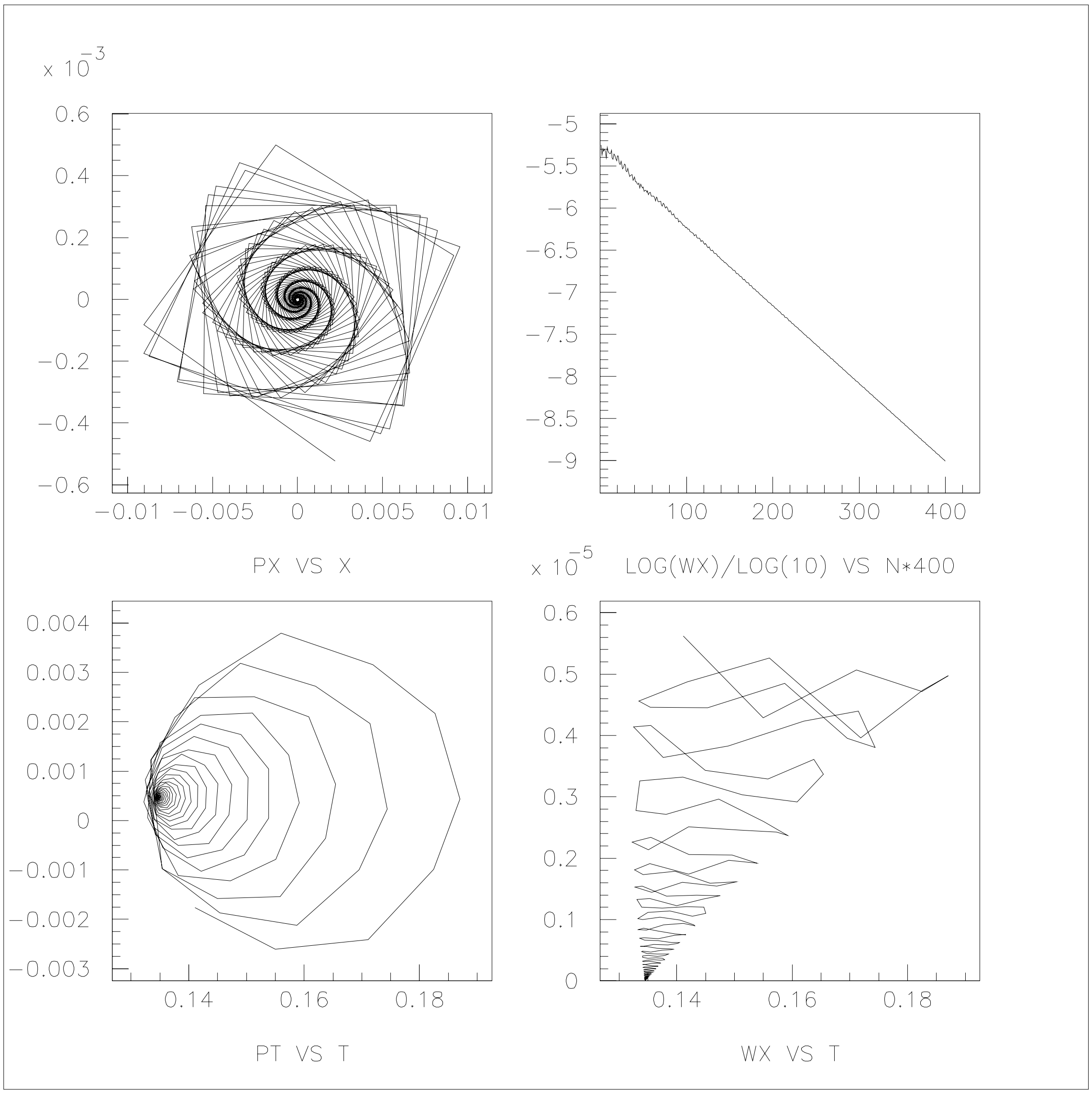

Figure 1.18: An example of Radiative Beta-synchrotron Coupling in tracking with damping. This is a LEP2 $90^\circ/60^\circ$ optics at 90 GeV. To guide the eye, the points representing the particle's coordinates on successive turns are joined by straight line segments. It starts off with a large horizontal betatron oscillation, A_x, but is otherwise on the closed orbit (in particular, the initial $A_t = 0$) and is followed for 400 turns. Motion in synchrotron phase space is generated out of the initial betatron oscillation. Both oscillations are damped away but the centre of the motion in synchrotron phase space shifts from the displaced to the stable phase.

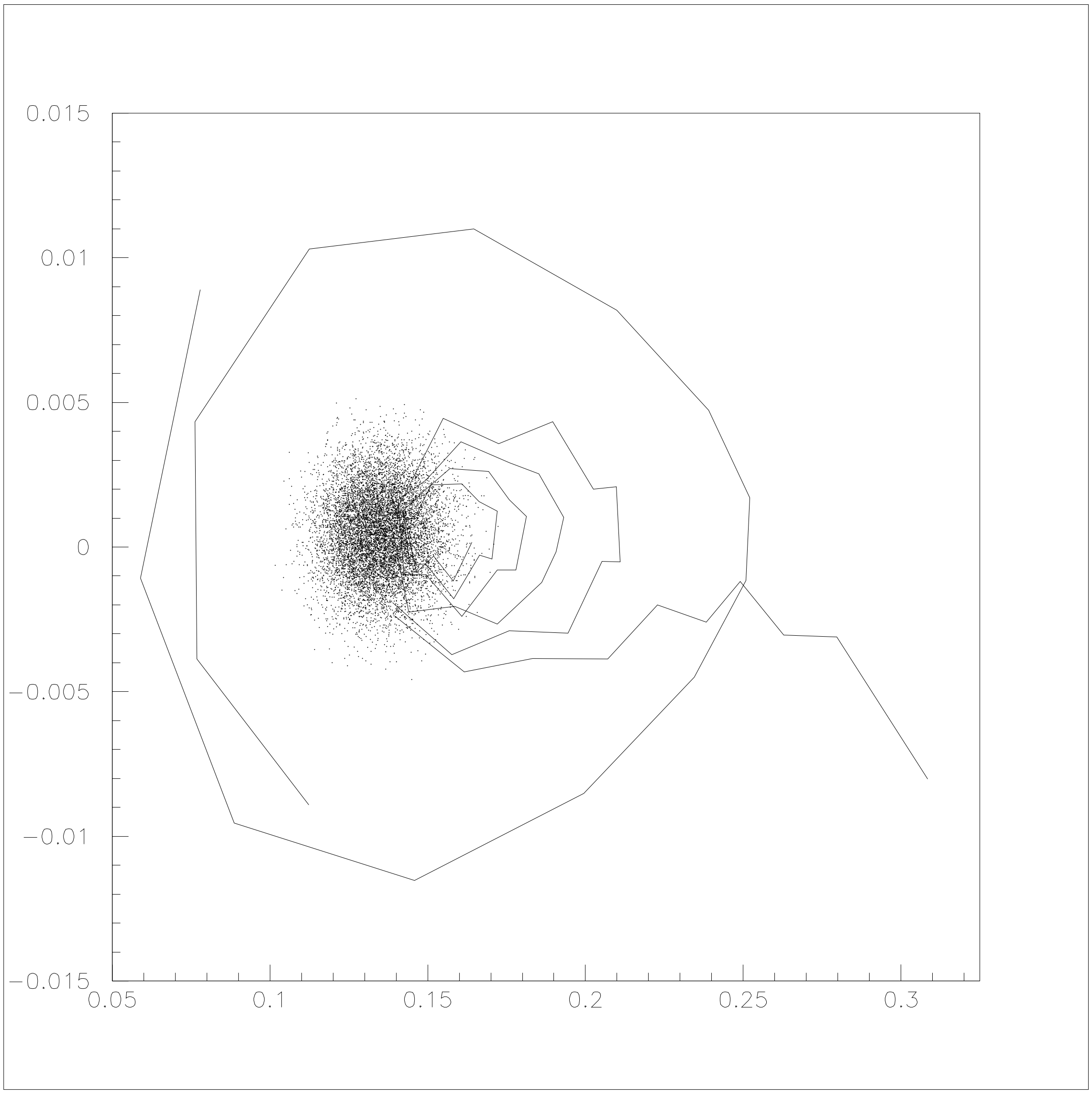

Figure 1.19: The Radiative Beta-synchrotron Coupling Instability. The conditions are similar to those described in Figure ??, except that here the continuous lines show the motion of two particles for 50 turns. One starts off with large A_t but remains stable and starts to damp to the stable phase. A second particle starts off with initial $y = 6\,\mathrm{mm}$, i.e., a large A_y (rather than A_x), and initial $A_t = 0$. Its amplitude grows until it is eventually lost. One particle has been tracked with quantum emission (for 10000 turns) to the cloud of points representing the core of the beam around the closed orbit.

- Other technical improvements and analytical tools provide better understanding of the physics.
- The outlook is for better accord between measurement and calculation.
- The dynamic aperture of the LEP2 optics appears just sufficient but there is very little margin. This is a major concern.
- An extensive programme of work remains to be tackled with these new tools:
  - Various optics (low-emittance and others).
  - Off-momentum orbits.
  - Pretzels (no reduction of dynamic aperture has been seen in tracking so far) and other separation schemes.
  - Misalignments and other imperfections.
  - Effects of RF station trips (work done with earlier versions of MAD is reported in [**?**]).
  - Further simulation of measurements (Q-meter, etc.)
  - Means to improve dynamic aperture need to be sought, especially in view of the small margin for LEP2.

Acknowledgements: The work described here was carried out together with François Barbarin and the collaboration of Chris Iselin in programming the changes to MAD. J.-P. Koutchouk, G. Roy and A. Verdier also provided valuable technical input.

References

[1] J.M. Jowett, "Introductory statistical mechanics for electron storage rings", Lectures given at the 5th US summer schools on Particle Accelerators, Stanford CA, 15–26 July 1985, SLAC PUB 4033 *and* M. Month and M. Dienes (Eds.), "Physics of particle Accelerators", US Summer School, SLAC, 1985, AIP Conference Proceedings 153 (1987) 864.

[2] M. Bassetti, "Effects due to the discontinuous replacement of radiated energy in an electron storage ring", Proc. 11th International conference on high-energy accelerators, Geneva, 7-11 July 1980, Birkhäuser, Basel, (1980) 650.

[3] Grote, H, Iselin, F.C., "The MAD program (methodical accelerator design) : version 8.10 ; user's reference manual", CERN SL 90–13 (AP) rev. 3 (1993).

[4] R.J. Noble, SLAC-PUB 3871 (1986).

[5] G. Roy, "A new method for the simulationm of synchrotron radiation in particle tracking codes", Nucl. Instruments and Methods, **A298** (1990) 128.

[6] F. Ruggiero, "Measurements vs. predictions of dynamic aperture", this workshop.

[7] F. Ruggiero, "Aperture Measurements" in J. Poole (Ed.), Proceedings of the Third Workshop on LEP Performance, Chamonix, January 10–16, 1993, CERN SL/93-19 (DI) (1993).

[8] F. Ruggiero, "Dynamic Aperture with RF Asymmetries", same proceedings as [**?**].